Ligand-induced Closure of Inward Rectifier Kir6.2 Channels Traps Spermine in the Pore

L. Revell Phillips and Colin G. Nichols

Department of Cell Biology and Physiology, Washington University School of Medicine, St. Louis, MO 63110

ABSTRACT Small organic amines block open voltage-gated K^+ channels and can be trapped by subsequent closure. Such studies provide strong evidence for voltage gating occurring at the intracellular end of the channel. We engineered the necessary properties (long block times with unblock kinetics comparable to, or slower than, the kinetics of gating) into spermine-blocked, ATP-gated (N160D,L157C) mutant K_{ATP} channels, in order to test the possibility of "blocker trapping" in ligand-gated Kir channels. Spermine block of these channels is very strongly voltage dependent, such that, at positive voltages, the off-rate of spermine is very low. A brief pulse to negative voltages rapidly relieves the block, but no such relief is observed in ATP-closed channels. The results are well fit by a simple kinetic model that assumes no spermine exit from closed channels. The results incontrovertibly demonstrate that spermine is trapped in channels that are closed by ATP, and implicate the M2 helix bundle crossing, or somewhere lower, as the probable location of the gate.

KEY WORDS: spermine • ATP • inward rectifier • gating • K channel

INTRODUCTION

The location of the "gates" in K^+ channels is of considerable topical interest. The static structures of several channels, as provided by crystallography (Doyle et al., 1998; Jiang et al., 2002a; Kuo et al., 2003), indicate two likely positions: in the selectivity filter or at the cytoplasmic end of the inner cavity that is formed by the four pore-lining helices (Fig. 1). Considerable evidence supports the notion that voltage gating of Shaker-like (Kv) channels occurs at the latter position (Holmgren et al., 1997, 1998; Liu et al., 1997; del Camino et al., 2000; del Camino and Yellen, 2001), as proposed for the gating of MthK and KcsA on the basis of the KcsA (closed) and MthK (open) crystal structures (Doyle et al., 1998; Jiang et al., 2002a,b). In ligand-gated channels, including those in the inward rectifier (Kir) channel family, the issue is currently much less clear. Consistent with a similar mechanism, mutations of residues at the lower end of M2 can "lock" Kir6.2 or Kir3 channels open (Enkvetchakul et al., 2001; Sadja et al., 2001; Yi et al., 2001), and introduction of prolines in this region can lock Kir3 channels essentially open or closed (Jin et al., 2002). In contrast, several studies indicate that accessibility of reagents or blockers to the inner cavity is not changed in the closed state (Bruening-Wright et al., 2002; Proks et al., 2003; Xiao et al., 2003), by default implicating the selectivity filter as the location of the gate. Our recent study of MTS-reagent accessibility in Kir6.2 channels indicates critical caveats to interpretation of such studies, and lead us to the conclusion that access to these reagents is gated by ATP and PIP_2 at or below the bundle crossing.

The notion of a gate at the cytoplasmic end of Kv channels is based on the classic "blocker trapping" experiments of Armstrong, who first examined the interaction of pore-blocking quaternary alkylamines with squid axon Kv channels (Armstrong, 1966, 1969, 1971; Holmgren et al., 1997; Liu et al., 1997). The present study was motivated to examine whether similar "blocker-trapping" occurs in ligand-gated Kir channels, and thereby test whether gating occurs above or below the blocker binding site. Such studies have not previously been performed on Kir channels, since in practice they require that blocker entry and exit rates be slower than, or at least on the same time scale, as gating itself. Such a situation rarely arises, since ligand gating tends to occur much more slowly than voltage gating. We took advantage of a mutant Kir6.2 (N160D) channel, in which the introduction of the negative charge in M2 renders the channel strongly rectifying, with measurable kinetics of spermine block and unblock (Shyng et al., 1997). At positive voltages, the spermine off-rate becomes significantly lower than rates of ATP gating, a necessary condition to reliably test for "trapping." The results incontrovertibly demonstrate that spermine is indeed trapped in its binding site, in channels that are closed by ATP. Spermine is released when the channels are opened by removal of ATP, or by application of PIP_2. Since spermine is a pore blocker that likely binds in the inner cavity of the

Address correspondence to Colin G. Nichols, Department of Cell Biology and Physiology, Washington University School of Medicine, 660 South Euclid Avenue, St. Louis, MO 63110. Fax: (314) 362-7463; email: cnichols@cellbio.wustl.edu

 J. Gen. Physiol. © The Rockefeller University Press • 0022-1295/2003/12/795/10 $8.00
Volume 122 December 2003 795–804
http://www.jgp.org/cgi/doi/10.1085/jgp.200308953

Kir channel (Loussouarn et al., 2002), the data imply that the ligand (ATP- or PIP_2-) -operated gate of Kir channels lies below the inner cavity, i.e., at or below the bundle crossing.

MATERIALS AND METHODS

Expression of K_{ATP} Channels in COSm6 cells

In all experiments Kir6.2 subunits were coexpressed with SUR1. COSm6 cells were plated at a density of $\sim 2.5 \times 10^5$ cells per well (30-mm 6-well dishes) and cultured in Dulbecco's modified eagle medium plus 10 mM glucose (DMEM-HG), supplemented with FCS (10%). On the first day after plating, cells were transfected using 1–2 μg each of pCMV6b-Kir6.2, pECE-SUR1, and pGreenlantern (GFP) (GIBCO BRL) and 5 μl FuGene6 (Roche Co.). 2 d after plating, transfected cells were replated onto glass coverslips for patch-clamping.

The primary channel constructs used were Kir6.2[N160D, L157C, C166S,Δ36] and Kir6.2[N160D, L164C, C166S,Δ36], referred to in results as N160D/L157C and N160D/L164C, respectively. The N160D mutation induces potent, steeply voltage-dependent block by spermine (see RESULTS). Similar trapping results were also seen in Kir6.2[N160D] channels without the C166S and L157C mutations, but the reported experiments were performed on the triple mutant subunits, as the L157C and C166S mutations raise the open state stability (Enkvetchakul et al., 2000), allowing patches to be studied for long periods of time without significant rundown of currents. These channel constructs also have a deletion of the last 36 amino acids from the COOH terminus (Δ36, Tucker et al., 1997). This removal of 36 amino acids has no effect on the function of channels coexpressed with SUR1 (as in all of the present experiments).

Patch-clamp Measurements

All experiments were performed at room temperature in a chamber that allowed the bathing solution exposed to the patch surface to be rapidly changed using an oil gate (Lederer and Nichols, 1989). Pipettes were pulled from Kimble 73813 soda lime glass using a horizontal puller (Sutter Instrument Co.). Electrode resistances ranged from 0.5 to 2.5 MΩ. Microelectrodes were sealed onto green fluorescing cells by applying light suction to the rear of the pipette. Inside-out patches were obtained by lifting the electrode and then passing the tip through the oil gate. Pipette and bath solutions contained a modified KINT (in mM 140 KCl, 1 EGTA, 1 EDTA, 4 K_2HPO_4, pH 7.4 with KOH), with additions as described. Membrane patches were voltage clamped using an Axopatch 1D amplifier. Currents were normally filtered at 1kHz and recorded directly onto a computer at 5 kHz using P-Clamp 7 and a digidata board (Axon Instruments, Inc.).

Dipotassium ATP and spermine were obtianed from Sigma-Aldrich, and stored as a powder at −20°C. ATP was made fresh each day in KINT and spermine was diluted from a 10M stock in KINT that was replaced at least monthly. PIP_2 (Roche Diagnostics) was stored as a stock solution at 1 mg/ml in water, then diluted to 5 μg/ml in experimental solutions and sonicated for 10 min in ice water before use.

Experimental Protocols for Analysis of Recovery from Spermine Block

Inside-out membrane patches are inevitably recessed within the electrode tip and instantaneous changes of bathing solution cannot be attained (Cannell and Nichols, 1991). Empirically we found that within a few seconds of spermine removal (at +40 mV), block was relieved by a brief negative pulse, but rapid reblock occurred on returning to positive voltages, making it difficult to assess the extent of recovery from block induced by the pulse. For quantitative analysis, we therefore used protocols like those in Fig. 2, in which the relieving voltage pulse was given at least 5 s after spermine removal. The rate of spermine washout was variable from patch to patch, with ∼75% of patches being fully washed out after 5 s. Patches with spermine washout times >5 s were not included in the analysis.

Data Analysis and Modeling

Off-line analysis was performed using Axon Clampfit and Microsoft Excel programs. Wherever possible, data are presented as mean ± SD, except where noted. Microsoft Solver was used to fit data by a least-square algorithm. Relative open probability (rPo), reported in some figures, was determined from current in the presence of ATP as a fraction of the current in zero ATP.

Markov models were assumed to be representative of actual K_{ATP} channel kinetics, and were used for simulations. Rate constants between states were constrained as described in the RESULTS section and microreversibility was observed. Time courses of occupancy of each state were calculated as described by Colquhoun and Hawkes (1995a,b). Specifically, the occupancy of each state at time t is given by $\mathbf{p}(t) = \mathbf{p}(0)e^{\mathbf{Q}t}$, where $\mathbf{p}(t)$ is a row vector with one element for each state in the model. $p(0)$ contains the occupancy probabilities of each state at t = 0 and was calculated from the equilibrium occupancy in the indicated [ATP]. Matrix $\mathbf{Q}$ was constructed with each element (i,j) equal to the rate constant from state i to state j, and elements (i,i) were set equal to the negative sum of all the other values in that row. The tasks of calculating rate constants, building the $\mathbf{Q}$ matrix, and solving for the above equations were performed either with MathCad6 (MathSoft), or with original programs written in Visual Basic or Visual Basic for Applications (Microsoft). The matrix exponential was calculated using either spectral expansion of a matrix, or by the Taylor series expansion of an exponential (Colquhoun and Hawkes, 1995a,b).

RESULTS

Voltage-dependent Spermine Block of N160D/L157C Channels

Classical "blocker-trapping" experiments, demonstrating that the blocker is trapped inside the pore by channel closure, require the blocker residency time to be measurable, and comparable to or slower than the rate of channel opening. Wild-type K_{ATP} channels are "weak" inward rectifiers, and show only weak, fast block by polyamines and other organic blockers. However, the introduction of a negative charge (N160D) into the M2 helices that line the inner pore renders them strong rectifiers that are blocked potently, and with very "strong" voltage dependence, by polyamines (Shyng et al., 1997). Fig. 1 indicates the location of mutations considered in this study. We used primarily Kir6.2[L157C,N160D,C166S,Δ36] (referred to as N160D/L157C) mutant channels in the following experiments. The L157C mutation stabilizes the open state, providing channel activity with no rundown of excised patch currents for many min-

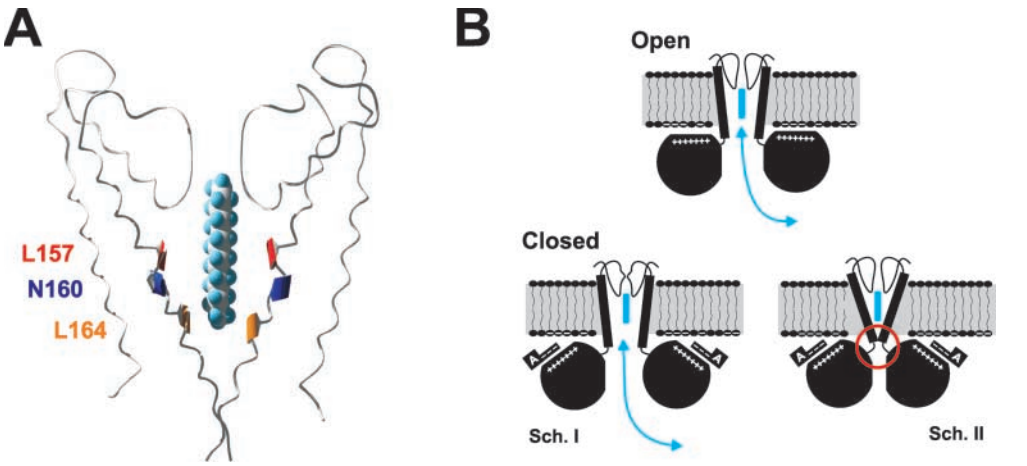

FIGURE 1. Location of possible gates in Kir6.2 channels. (A) Cartoon showing a likely pore structure for Kir6.2 (model based on KcsA; Loussouarn et al., 2000). Backbone locations of critical residues mutated in the present study are indicated. Also shown is a space-filling model of the elongated form of spermine, placed in a likely blocking location in the pore axis. (B) Models for channel gating. In each case, spermine has voltage-dependent access to its binding site in the open state, but in the ATP-closed state may still access the binding site if gating occurs at the selectivity filter (Scheme I), or has no access if gating occurs at, or more cytoplasmically to, the M2 helix bundle crossing (Scheme II).

utes, allowing for the long protocols required in the following experiments.

Fig. 2 illustrates the voltage dependence and kinetics of spermine block in N160D/L157C channels. 10 μM spermine causes complete block of channel currents at positive voltages, with steep voltage dependence (Fig. 2, A and B). The relative conductance-voltage relationship is well fit by a single Boltzmann function (Fig. 2 C) and current relaxations are monoexponential, both for block and unblock (Fig. 2 D). Accordingly, we fitted exponential functions to current relaxations (Fig. 2 D) and estimated voltage-dependent on- and off-rates for a simple 2-state model (Fig. 2 E).

$$O_B \underset{k_{In}(v).[s]}{\overset{k_{Out}(v)}{\rightleftharpoons}} O$$

SCHEME I

The model reproduces the observed voltage dependence of spermine block, with $k_{in}(0) = 1.30\ \mu M^{-1}.s^{-1}$, $z_{in} = 1.95$, and $k_{out}(0) = 1.3\ s^{-1}$, $z_{out} = 2.1$.

Measurements of off-rates using concentration "jump" experiments in inside-out membrane patches are always compounded by limited diffusion rates out of the recessed patch (Cannell and Nichols, 1991), but at positive voltages, the predicted spermine off-rate (Fig. 2 E) becomes extremely slow. It should thus be possible to determine the unidirectional spermine off-rate after removal of spermine from the solution (Fig. 3 A) with minimal contribution of diffusion. The measured time constant of spermine unblock at +40 mV of 10–30 s (Fig. 3 A) compares well to that predicted from the model ($k_{out}(+40) = 0.05\ s^{-1}$, $\tau_{out} = 20.0$ s, Fig. 2 E). Brief (10 ms) pulses to a series of voltages more negative than −20 mV rapidly relieve the block (Fig. 3 A, expanded time scale to right). The relative recovery is plotted as a function of pulse voltage in Fig. 3 B. The data are well predicted by the voltage-dependent k_{out} estimated for the 2-state model (red line, Fig. 3 B). We have also examined the time dependence of current relief at −40 mV (Fig. 3 C). After removal of spermine (at +40 mV), the potential was stepped briefly back to −40 mV for variable times. The relative recovery is plotted as a function of pulse duration (Fig. 3 D) from multiple similar experiments. Again, the time course of recovery is well predicted by the simple 2-state model (red line) of spermine block, using rate constants as determined in Fig. 2. In the following experiments, we have collected data on the recovery from spermine block in channels closed by ATP, and have extended the analysis of this two-state model to incorporate channel gating.

Spermine Is Trapped in ATP-closed Channels

Fig. 4 A shows current records from a patch expressing N160D/L157C channels, with exposure to spermine and ATP as indicated. At +40 mV, channels are blocked rapidly and completely by 10 μM spermine. After spermine removal from the solution, unblock is extremely slow (tau ~30 s, trace 1). However, block is rapidly and completely relieved by a brief (300 ms) pulse to −40 mV (trace 2). N160D/L157C channels are >95% closed by 10 mM ATP (Enkvetchakul et al., 2000). As shown in trace 3, when spermine-blocked channels are subsequently exposed to ATP, a 300 ms pulse to −40 mV now completely fails to relieve spermine block, as evidenced by unaltered subsequent time course of spermine release, after ATP is removed (compare trace 3 to trace 1).

The above experiment indicates that ATP traps spermine in the pore, the simplest interpretation being

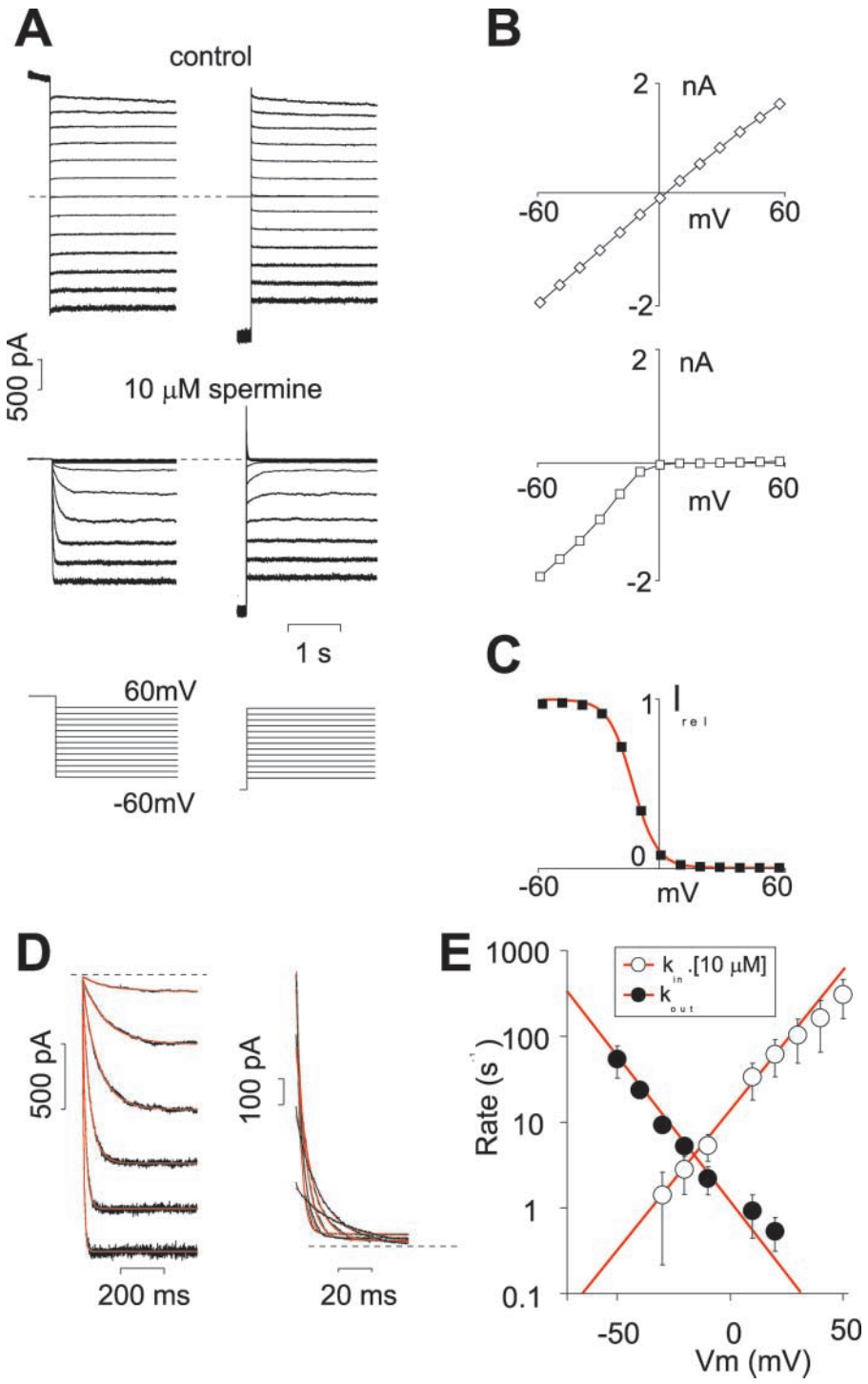

FIGURE 2. Voltage-dependent block of N160D/L157C channels by spermine. (A) Representative inside-out current records in the absence and presence of 10 μM spermine, in response to voltage steps from $V_h = -60$ mV to voltages between −60 and +60 mV (10-mV steps). (B) Steady-state current-voltage relationships (from A). (C) Relative conductance (I_{rel})-voltage relationships computed from above ($I_{rel} = I_{spermine}/I_{cont}$), fit with Boltzmann function ($Z = 4.04$, $V_{1/2} = -14.4$ mV). (D) Expanded time base records of current in the presence of spermine, in response to voltage steps from +60 mV to voltages between −10 and −60 mV (left), or from −60 mV to voltages between +10 and +60 mV (right), with single exponential fits indicated. (E) Spermine entry ($k_{in} \times$ [spermine]) and exit (k_{out}) rates as a function of V_m, estimated from current relaxation kinetics (D) and steady-state block (C) by 10 μM spermine (see text).

that ATP does so by closing the channels. To exclude alternative possible consequences of ATP binding, the experiment was repeated on an additional mutant channel. In contrast to N160D/L157C channels, N160D/L164C channels, with a cysteine substituted at residue 164, bind ATP but have an extremely high open state stability and are not closed by 10 mM ATP (Enkvetchakul et al., 2000, 2001). In Fig. 4 B, the above experiment was repeated on a patch containing N160D/L164C channels. After the removal of spermine from solution, spermine block is rapidly and completely relieved by a brief (100 ms) pulse to −40 mV (trace 2). In contrast to N160D/L157C channels, block of N160D/L164C channels is still fully relieved when the 100-ms pulse is applied during exposure to 10 mM ATP (trace 3). That ATP traps spermine in

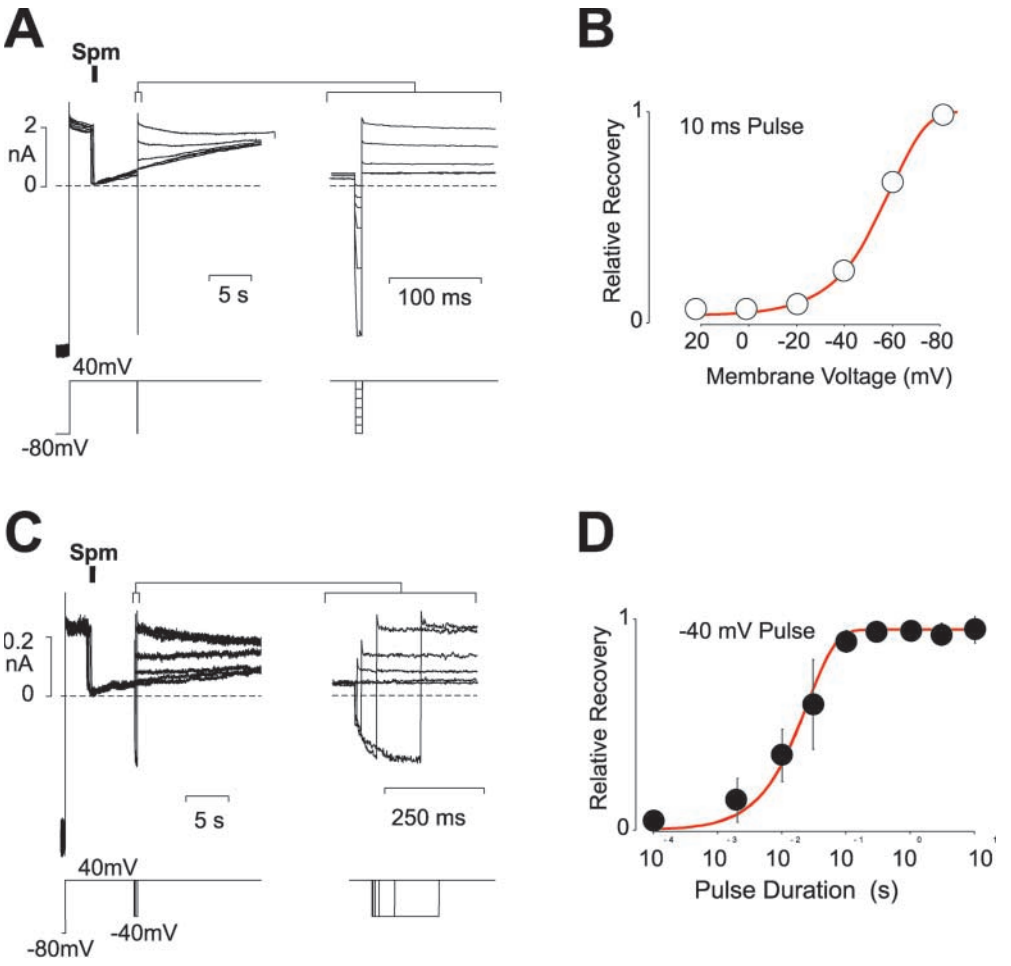

FIGURE 3. Spermine unblock rates estimated using "concentration jump." (A) Spermine (10 μM) was briefly applied (as indicated) to block all channels at +40 mV. After spermine removal, currents recover slowly (τ ~20 s). Brief pulses to voltages more negative than −20 (left and expanded) significantly relieve inhibition. (B) Relative recovery of current is plotted versus pulse voltage. The solid red line indicates the predicted recovery given the spermine off-rate (k_{out}) calculated in Fig. 2. (C) Spermine (10 μM) was briefly applied (as indicated) to block all channels at +40 mV. After spermine removal, pulses to −40 mV were applied for various durations. (D) Relative recovery of current is plotted versus pulse duration for four similar experiments (mean ± SEM). The solid red line indicates the predicted recovery given the spermine off-rate calculated in Fig. 2.

N160D/L157C channels (Fig. 4 A), but not in N160D/L164C channels (Fig. 4 B), indicates that spermine trapping in the former is due to channel closure, and not some other effect of ATP.

Quantitative Predictions with Incorporation of Gating: Trapping Is Complete

To gain further quantitative insight to the extent of trapping in closed channels, we performed experiments as shown in Fig. 5. In Fig. 5 A, N160D/L157C channels were blocked by spermine at +40 mV, then closed in 10 mM ATP, and stepped to −40 mV for variable durations, before subsequent removal of ATP. For each patch, the current in ATP was estimated relative to the current in the absence of ATP. This is expressed as a relative open probability (rPo). In this patch the current was inhibited 90% in ATP (i.e., rPo = 0.10). The relative recovery from spermine block (assessed as indicated in the figure) was plotted against pulse duration (Fig. 5 B). The detailed kinetics of ATP-gating of K_{ATP} channels are complex (Enkvetchakul et al., 2000), but for the current purpose of assessing the degree of trapping in closed channels, even a simplified 2-state model of gating provides a very unambiguous answer. Fig. 5 B shows the predicted recovery from spermine block in open channels and in partially ATP–closed channels for two extreme cases: (1) in which spermine can access its binding site in both open and closed channels (Scheme I), and (2) in which access is limited only to open channels (Scheme II):

[I] [II]

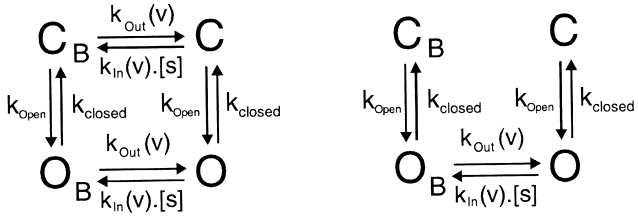

SCHEME II

O and C represent open and closed states, O_B and C_B represent open, blocked and closed, blocked states, and k_x represents the relevant voltage-, [ATP]-, or [spermine]-dependent rate constants. To model the time course of recovery from block upon removal of

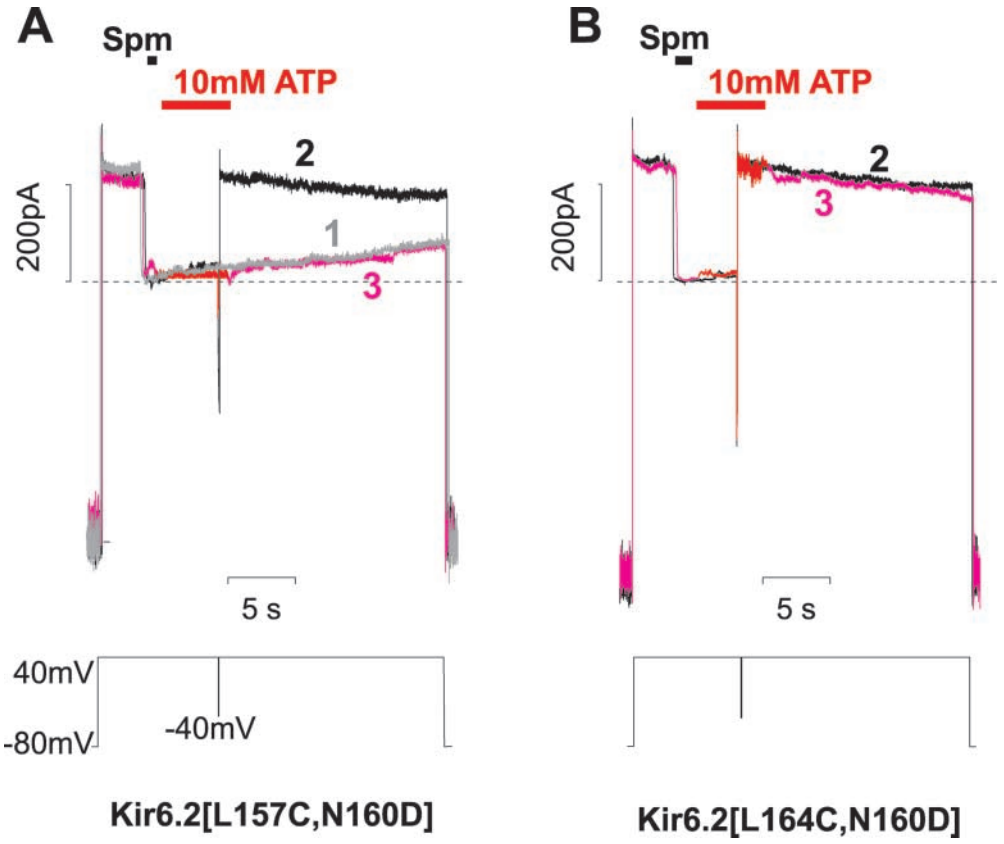

FIGURE 4. ATP closure traps spermine in the channel. (A) Spermine (10 μM) was briefly applied (as indicated) to block N160D/L157C channels at +40 mV. After spermine removal, currents recover slowly (trace 1). In trace 2, after spermine removal, a 300-ms pulse to −40 mV completely relieves block. In trace 3, channels were exposed to 10 mM ATP after spermine removal. A 300-ms pulse to −40 mV was applied, then ATP removed. In the ATP closed channels, there is no recovery from spermine block. (B) In trace 2, spermine (10 μM) was briefly applied (as indicated) to block Kir6.2[L164C, N160D] channels at +40 mV. After spermine removal, a 100-ms pulse to −40 mV completely relieves block. In trace 3, channels were exposed to 10 mM ATP following spermine removal. In contrast to N160D/L157C channels, ATP fails to close N160D/L164C channels, and a 100-ms pulse to −40 mV applied during ATP exposure fails to protect against spermine release (representative experiment, $n = 3$).

spermine in ATP (e.g., as in Figs. 4, and 5 A) these schemes reduce to:

[Ir] [IIr]

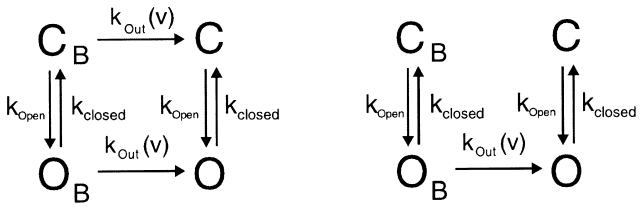

SCHEME III

Superimposed in Fig. 5 B are the predictions of Schemes Ir and IIr, with the following rate constants (see Fig. 5 C): k_{out} (−40) = 28 s^{-1}, k_{open} = 0.33 s^{-1}. This opening rate approximates the lumped kinetics of K_{ATP} channel opening that are typically observed in excised patch recordings (Qin et al., 1989; Nichols et al., 1991). The closing rate ($k_{closed} = k_{open}.[1 - P_o)/P_o]$), was then calculated to give the appropriate open probability (P_o). In the particular patch illustrated in Fig. 5 B, the estimated relative open probability in 10 mM ATP was 0.10, and curves are predicted for the two schemes, with P_o= 1 (k_c = 0 s^{-1}) and 0.1 (k_c = 2.7 s^{-1}). The ungated access model (Ir) predicts no slowing of recovery in partially closed channels, and the observed time course of recovery is well predicted by the fully gated access model (Iir).

Varying Open State Stability by Changing PIP_2 Shifts the ATP-trapping Efficacy: PIP_2 and ATP Act on the Same Gate

The above results argue that spermine cannot exit channels that are closed by ATP. Exogenous application of PIP_2 leads to increased open state stability of K_{ATP} channels, and thereby increases open probability at any given [ATP] (Baukrowitz et al., 1998; Shyng and Nichols, 1998; Enkvetchakul et al., 2000, 2001). This is consistent with ATP and PIP_2 acting on the same "gate," and Fig. 5 C shows the results of an experiment designed to test whether PIP_2 can similarly counter the spermine-trapping effects of ATP. Before treatment with PIP_2, 10 mM ATP inhibited current in this particular patch to rPo ~0.1, and on exposure to a 1-s pulse to −40 mV, trapping of spermine was essentially complete. The patch was subsequently exposed to PIP_2, until rPo in 10 mM ATP was increased to ~0.5. Upon repeating

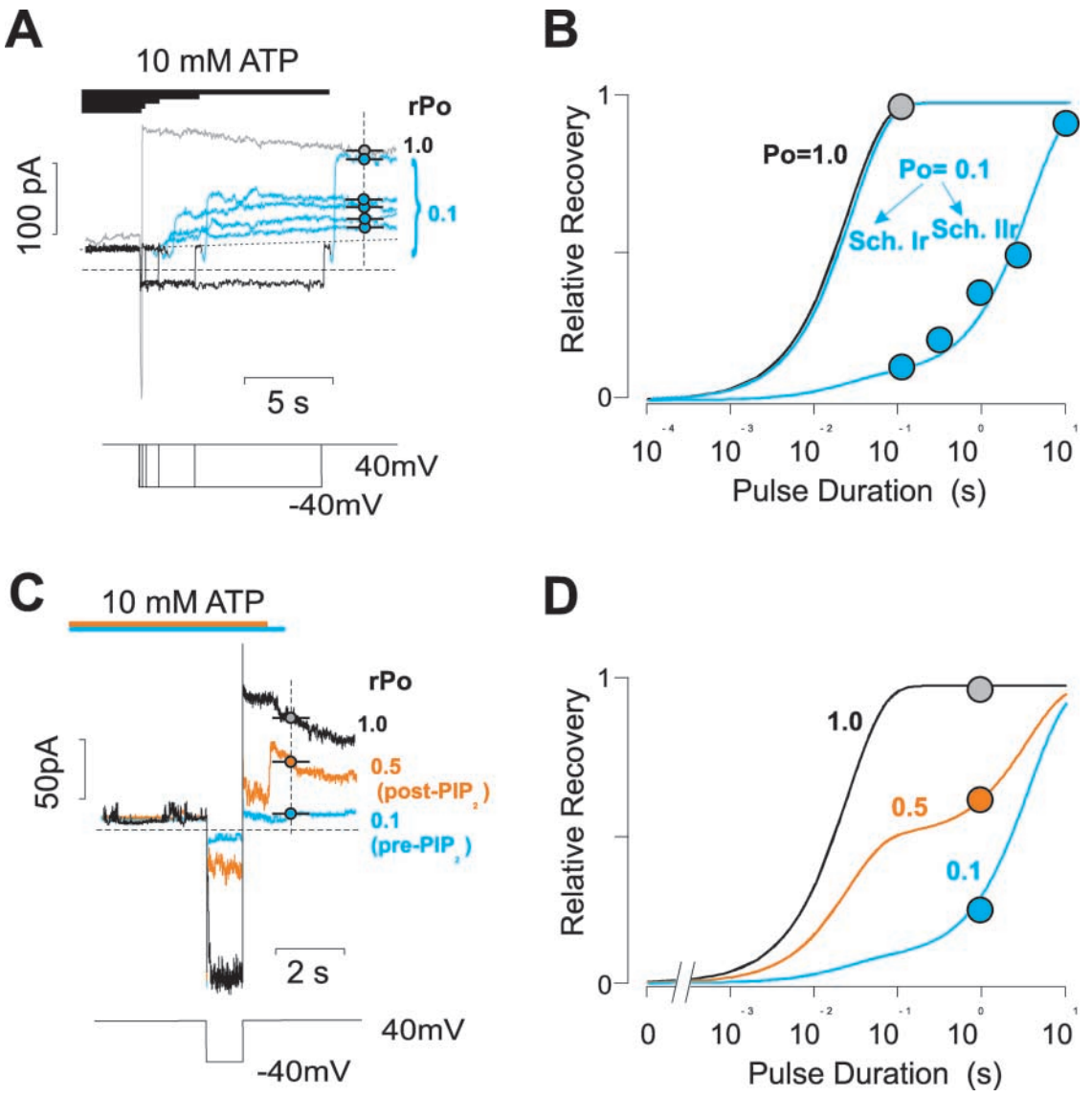

FIGURE 5. ATP traps spermine in closed channels. (A) Spermine (10 μM) was briefly applied to block N160D/L157C channels at +40 mV, and then spermine was removed ~2 s before the onset of the recorded traces and the patch was exposed to 10 mM ATP (rPo = 0.10) at the onset of each recording. Variable duration pulses to −40 mV were applied. ATP was subsequently removed, and the extent of recovery assessed as indicated (current was averaged for 1 s at dashed vertical line). Shown in gray is the response to a 100-ms pulse to −40 mV without exposure to ATP (rPo = 1.0). This completely relieves block in open channels. (B) Relative recovery of current is plotted versus pulse duration (from the experiment in A). The solid lines indicate the predicted recovery for Po = 1.0 and Po = 0.1 for Schemes I and II (see text). (C) Spermine (10 μM) was briefly applied to block N160D/L157C channels at +40 mV, and then spermine was removed ~2 s before the onset of the recorded traces. A 1-s pulse to −40 mV completely relieves block of open channels (rPo = 1.0, black trace). The protocol was repeated and, after removal of spermine, the patch was exposed to 10 mM ATP (blue trace, rPo ~0.1) at the beginning of the recording. A 1-s pulse to −40 mV was applied and recovery assessed as indicated. The patch was then exposed to 5 mg/ml PIP_2 for ~1 min to increase channel open state stability. Exposure to PIP_2 increased rPo in 10 mM ATP to ~0.5. The patch was again blocked by spermine (10 μM) and, after spermine removal, the patch was exposed to 10 mM ATP (orange trace, rPo = 0.50), and a 1-s step to −40 mV was applied and recovery assessed as indicated. (D) Relative recovery of current is plotted versus pulse duration. The solid lines indicate the predicted recovery for Po for Scheme II (see text). The trapping effect of ATP is antagonized by PIP_2.

the trapping protocol, a 1-s pulse to −40 mV now resulted in much greater relief of spermine block (orange trace), consistent with PIP_2-induced destabilization of the ATP-induced closure (Enkvetchakul et al., 2000). Fig. 5 D shows the predictions of Scheme IIr, with the rate constants used in Fig. 5 B, superimposed on the estimated fractional recovery from each of the traces in Fig. 5 C. Again, the dependence of the observed time course of recovery on open probability is well predicted by the fully gated access model (Scheme IIr).

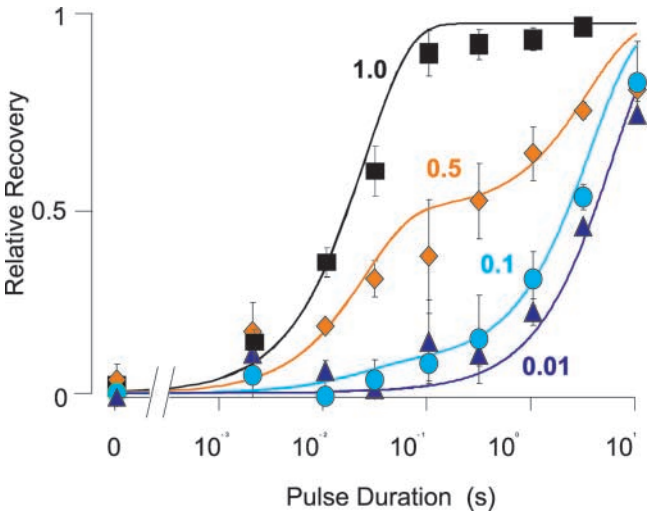

FIGURE 6. Spermine trapping depends on open probability. Relative recovery of current is plotted versus pulse duration for multiple similar experiments of the kind shown in Fig. 5. Data from experiments (as in Fig. 5, A and C) were pooled by rPo, without regard to applied [ATP] and without regard to prior exposure to PIP_2. The solid lines indicate the predicted recovery for Po as indicated from Scheme II (see text). The pooled data correspond to rPo = 1, $n = 12$ (black symbols); rPo = 0.49 ± 0.06, $n = 4$ (orange symbols); rPo = 0.09 ± 0.01, $n = 5$ (blue symbols); rPo = 0.013 ± 0.005, $n = 3$ (purple symbols).

From multiple experiments like those in Fig. 5, we were able to estimate the recovery timecourse (at −40 mV) during exposure to different concentrations of ATP, with or without PIP_2 treatment (and hence at different open probabilities). Datasets were pooled by estimated relative open probability (rPo) in ATP. The data are plotted in Fig. 6, together with the predictions of Scheme II for each Popen. There is a biphasic recovery from block, and as Popen changes, the weighting of each phase shifts. The consistent quantitative agreement between data and model argues strongly that trapping of spermine is essentially complete in closed channels.

DISCUSSION

Gated Access of both Cysteine Modifiers and Polyamines to the Kir Inner Cavity

Our previous analysis of gating dependence of MTSEA modification of cysteines in the inner pore of Kir6.2 channels (Phillips et al., 2003) illustrated a complex voltage and gating dependence of overall modification rates that led to us to propose ligand-gated access, i.e., that MTSEA cannot enter the ligand-closed channel, and hence that the ligand-operated gate lies below the inner pore (Jiang et al., 2002a,b). The present demonstration of spermine trapping in closed channels is a more direct demonstration of gated access to the pore, providing clear evidence that the polyamine cannot escape from its binding site, when channels are in the ligand-closed state. These experiments are similar to the classical blocker-trapping experiments of Armstrong (1966, 1969, 1971) that first led to the suggestion that voltage gating of Kv channels occurs by closure of a "gate," located near the cytoplasmic end of the channel, now postulated to be at the bundle crossing of the S6 (M2) helices (Jiang et al., 2002a,b). Such experiments have not been performed previously in inward rectifier channels, since the necessary conditions (long block times providing unblock kinetics that are comparable to, or slower than, the kinetics of gating) are rarely encountered. These conditions are met in the present experiments by the very stable spermine block of a strong inward rectifying channel having relatively rapid ligand (ATP) gating.

There is currently some controversy regarding the binding site of polyamines in Kir channels. Based on the crystal structure of the cytoplasmic domain of Kir3 channels, Guo and colleagues (Guo and Lu, 2003; Guo et al., 2003) recently proposed that polyamines bind peripherally in the cytoplasmic portion of the pore and extend into the inner cavity. There is considerable evidence from other mutational analyses that, while polyamines may bind in the cytoplasmic pore to reduce single channel conductance, the high-affinity binding site responsible for classic strong inward rectification lies in or above the inner cavity (Lu and MacKinnon, 1994; Kubo and Murata, 2001; Xie et al., 2002). Either way, the present results argue that, to trap spermine, the ligand-operated gate would have to be at or below the inner cavity. Spermine block of N160D/L157C channels is well fit by a simple 2-state model with concentration- and voltage-dependent binding to a single site (Fig. 2). The overlapping, weakly voltage-dependent additional component of spermine inhibition that can be prominent in Kir2.1 and Kir2.3 channels (Lopatin et al., 1995; Xie et al., 2002, 2003) is not evident in these channels at low micromolar concentrations, greatly simplifying the present analysis. We can thus argue that because channel closure traps a single spermine molecule in the pore, the ligand-operated gate in Kir6.2 likely lies below the inner cavity. That the trapping by ATP closure of the channels is antagonized by PIP_2 is entirely consistent with the view that it is the same "gate" which is stabilized in the closed state by ATP, and in the open state by PIP_2 (Baukrowitz et al., 1998; Shyng and Nichols, 1998; Enkvetchakul et al., 2000, 2001).

Comparison to other Studies

There is now mounting structural and biophysical evidence that the voltage (or ligand) -operated gate of voltage-gated, or Ca-gated K^+ channels corresponds to

a pinching of the permeation pathway by the M2 helix bundle crossing, as a result of hinged motion of M2 at a conserved glycine (G156 in Kir6.2) residue in the center of M2 (Doyle et al., 1998; del Camino and Yellen, 2001; Jiang et al., 2002a,b; Rothberg et al., 2002). The structure of a bacterial Kir channel (KirBac1.1) pore demonstrates a similar structure in Kir channels (Kuo et al., 2003). These authors argue that hinged gating may not occur at the equivalent glycine residue, but there are parallel consequences of M2 (S6) mutations on open state stability of Kir and Kv channels (Holmgren et al., 1998; Enkvetchakul et al., 2000, 2001; Espinosa et al., 2001; Yi et al., 2001; Hackos et al., 2002).

We have now provided direct evidence for gated access to inner cavity residues in Kir6.2 (Phillips et al., 2003), but other recent studies have questioned the interpretation that the ligand-operated gate of Kir channels lies at or below the bundle crossing of the M2 helices, instead suggesting that gating must occur much higher, i.e., In the selectivity filter (Proks et al., 2003; Xiao et al., 2003). In particular, these latter studies reach conclusions that are not easily reconciled with those of either the present or our previous accessibility study. Proks et al. (2003) examined the rate of block of Kir6.2 channels by cytoplasmic Ba^{2+} after depolarizing pulses and provided evidence for a speeding up of the Ba^{2+} block rate in partially ATP-closed channels. We have repeated their experiment with wild-type Kir6.2+SUR1 channels in essentially identical conditions. After scaling the currents to the prepulse current (rather than the peak current which can be contaminated by large capacitance artifacts), we observe no significant change in the rapid phase of Ba^{2+} block. However, we do observe a significant, very slow ($t \sim 1$–3 s), component of Ba^{2+} block that is only present in ATP. This slow phase of block might be due to a gated access (i.e., if a fraction of channels must open from long lived closed states before blocking). In another study examining gating dependence of pore access in Kir channels, Xiao et al. (2003) demonstrated no slowing of the MTSEA accessibility of M2 cysteines in Kir2.1 channels that were closed by reducing membrane PIP_2 levels. The kinetics of MTSEA modification of equivalent M2 residues in open Kir6.2 channels (Phillips et al., 2003) are very similar to those in Kir2.1 channels (Xiao et al., 2003) and, given the potential caveats of reagent trapping described in the former study, it is unclear whether the necessary degree of closure or appropriate gating kinetics were present to uncover a true gating dependence of access in the latter.

Consistent with a gated access to the inner cavity, we demonstrated previously that Cd^{2+} coordination by cysteines in M2 is reduced in closed Kir6.2 channels (Loussouarn et al., 2000). Xiao et al. (2003) reported similar slowing of Cd^{2+} block in closed Kir2.1 channels with substituted cysteines in M2, but only marginal slowing of Ag modification of M2 residues in closed channels. Considering a simplified model of gated access, Xiao et al. (2003) concluded that reagent trapping could not account for this result, and suggested that access to the inner cavity for Ag^+ ion (and hence for the similar-sized K^+ ion) is not gated. It remains conceivable that a closure of the bundle crossing, sufficient to trap spermine in the pore or to exclude MTS reagents, is insufficient to exclude Ag^+ or K^+ ions, but it is disconcerting that Xiao et al. (2003) also reported very rapid modification of M1 residues (that obviously do not line the permeation pathway) by Ag^+ ions.

Conclusions

The present data demonstrate unequivocally that classic pore blocker trapping by channel closure can be observed in inward rectifier channels; trapping of spermine ions in closed channels is essentially complete. Although we cannot formally exclude a model whereby a closure at the selectivity filter somehow traps spermine in the filter itself, nor the possibility that the "gate" to spermine exit is distinct from the gate to K^+ ions, the simplest interpretation is that ATP stabilizes the closing (and PIP_2 stabilizes the opening) of a gate that is located intracellular to the spermine binding site. Since the spermine binding site is likely to be in the inner cavity, this would localize the gate to the M2 helix bundle crossing or below.

We thank the Washington University Diabetes Research and Training Center for reagent support. We are grateful to Dr. D. Enkvetchakul for help with implementing kinetic models and Drs. C. Lingle and J. Huettner for critical discussion.

This work was supported by Grants HL54171 (to C.G. Nichols) from the National Institutes of Health, and the National Institutes of Health Biophysical Training grant at Washington University (predoctoral support of L.R. Phillips).

Olaf S. Andersen served as editor.

Submitted: 24 September 2003
Accepted: 31 October 2003

REFERENCES

Armstrong, C.M. 1966. Time Course of TEA(+)-induced Anomalous Rectification in Squid Giant Axons. *J. Gen. Physiol.* 50:491–503.

Armstrong, C.M. 1969. Inactivation of the potassium conductance and related phenomena caused by quaternary ammonium ion injection in squid axons. *J. Gen. Physiol.* 54:553–575.

Armstrong, C.M. 1971. Interaction of tetraethylammonium ion derivatives with the potassium channels of giant axons. *J. Gen. Physiol.* 58:413–437.

Baukrowitz, T., U. Schulte, D. Oliver, S. Herlitze, T. Krauter, S.J. Tucker, J.P. Ruppersberg, and B. Fakler. 1998. PIP2 and PIP as determinants for ATP inhibition of KATP channels. *Science.* 282: 1141–1144.

Bruening-Wright, A., M.A. Schumacher, J.P. Adelman, and J. May-

lie. 2002. Localization of the activation gate for small conductance Ca^{2+}-activated K+ channels. *J. Neurosci.* 22:6499–6506.
Cannell, M.B., and C.G. Nichols. 1991. Effects of pipette geometry on the time course of solution change in patch clamp experiments. *Biophys. J.* 60:1156–1163.
Colquhoun, D., and A.G. Hawkes. 1995a. The principles of the stochastic interpretation of ion-channel mechanisms. *In* Single-channel Recording. B. Sakmann and E. Neher, editors. Plenum Press, New York. 397–482.
Colquhoun, D., and A.G. Hawkes. 1995b. A Q-matrix cookbook: how to write only one program to calculate the single-channel and macroscopic predictions for any kinetic mechanism. *In* Single-channel Recording. B. Sakmann and E. Neher, editors. Plenum Press, New York. 589–636.
del Camino, D., M. Holmgren, Y. Liu, and G. Yellen. 2000. Blocker protection in the pore of a voltage-gated K+ channel and its structural implications. *Nature.* 403:321–325.
del Camino, D., and G. Yellen. 2001. Tight steric closure at the intracellular activation gate of a voltage-gated k(+) channel. *Neuron.* 32:649–656.
Doyle, D.A., J. Morais Cabral, R.A. Pfuetzner, A. Kuo, J.M. Gulbis, S.L. Cohen, B.T. Chait, and R. MacKinnon. 1998. The structure of the potassium channel: molecular basis of K+ conduction and selectivity. *Science.* 280:69–77.
Enkvetchakul, D., G. Loussouarn, E. Makhina, and C.G. Nichols. 2001. ATP interaction with the open state of the K(ATP) channel. *Biophys. J.* 80:719–728.
Enkvetchakul, D., G. Loussouarn, E. Makhina, S.L. Shyng, and C.G. Nichols. 2000. The kinetic and physical basis of K(ATP) channel gating: toward a unified molecular understanding. *Biophys. J.* 78: 2334–2348.
Espinosa, F., R. Fleischhauer, A. McMahon, and R.H. Joho. 2001. Dynamic interaction of S5 and S6 during voltage-controlled gating in a potassium channel. *J. Gen. Physiol.* 118:157–170.
Guo, D., and Z. Lu. 2003. Interaction mechanisms between polyamines and IRK1 inward rectifier K^+ channels. *J. Gen. Physiol.* 122:485–500.
Guo, D., Y. Ramu, A.M. Klem, and Z. Lu. 2003. Mechanism of rectification in inward-rectifier K^+ channels. *J. Gen. Physiol.* 121:261–276.
Hackos, D.H., T.H. Chang, and K.J. Swartz. 2002. Scanning the intracellular s6 activation gate in the Shaker K^+ channel. *J. Gen. Physiol.* 119:521–532.
Holmgren, M., K.S. Shin, and G. Yellen. 1998. The activation gate of a voltage-gated K^+ channel can be trapped in the open state by an intersubunit metal bridge. *Neuron.* 21:617–621.
Holmgren, M., P.L. Smith, and G. Yellen. 1997. Trapping of organic blockers by closing of voltage-dependent K^+ channels - evidence for a trap door mechanism of activation gating. *J. Gen. Physiol.* 109:527–535.
Jiang, Y., A. Lee, J. Chen, M. Cadene, B.T. Chait, and R. MacKinnon. 2002a. Crystal structure and mechanism of a calcium-gated potassium channel. *Nature.* 417:515–522.
Jiang, Y., A. Lee, J. Chen, M. Cadene, B.T. Chait, and R. MacKinnon. 2002b. The open pore conformation of potassium channels. *Nature.* 417:523–526.
Jin, T., L. Peng, T. Mirshahi, T. Rohacs, K.W. Chan, R. Sanchez, and D.E. Logothetis. 2002. The βγ subunits of G proteins gate a K^+ channel by pivoted bending of a transmembrane segment. *Mol. Cell.* 10:469–481.
Kubo, Y., and Y. Murata. 2001. Control of rectification and permeation by two distinct sites after the second transmembrane region in Kir2.1 K^+ channel. *J. Physiol.* 531:645–660.
Kuo, A., J.M. Gulbis, J.F. Antcliff, T. Rahman, E.D. Lowe, J. Zimmer, J. Cuthbertson, F.M. Ashcroft, T. Ezaki, and D.A. Doyle. 2003. Crystal structure of the potassium channel KirBac1.1 in the closed state. *Science.* 300:1922–1926.
Lederer, W.J., and C.G. Nichols. 1989. Nucleotide modulation of the activity of rat heart ATP-sensitive K^+ channels in isolated membrane patches. *J. Physiol.* 419:193–211.
Liu, Y., M. Holmgren, M.E. Jurman, and G. Yellen. 1997. Gated access to the pore of a voltage-dependent K^+ channel. *Neuron.* 19: 175–184.
Lopatin, A.N., E.N. Makhina, and C.G. Nichols. 1995. The mechanism of inward rectification of potassium channels—long-pore plugging by cytoplasmic polyamines. *J. Gen. Physiol.* 106:923–955.
Loussouarn, G., E.N. Makhina, T. Rose, and C.G. Nichols. 2000. Structure and dynamics of the pore of inwardly rectifying K(ATP) channels. *J. Biol. Chem.* 275:1137–1144.
Loussouarn, G., T. Rose, and C.G. Nichols. 2002. Structural basis of inward rectifying potassium channel gating. *Trends Cardiovasc. Med.* 12:253–258.
Lu, Z., and R. MacKinnon. 1994. Electrostatic tuning of Mg^{2+} affinity in an inward-rectifier K+ channel. *Nature.* 371:243–246.
Nichols, C.G., W.J. Lederer, and M.B. Cannell. 1991. ATP dependence of KATP channel kinetics in isolated membrane patches from rat ventricle. *Biophys. J.* 60:1164–1177.
Phillips, L.R., D. Enkvetchakul, and C.G. Nichols. 2003. Gating dependence of inner pore access in inward rectifier K(+) channels. *Neuron.* 37:953–962.
Proks, P., J.F. Antcliff, and F.M. Ashcroft. 2003. The ligand-sensitive gate of a potassium channel lies close to the selectivity filter. *EMBO Rep.* 4:70–75.
Qin, D.Y., M. Takano, and A. Noma. 1989. Kinetics of ATP-sensitive K^+ channel revealed with oil-gate concentration jump method. *Am. J. Physiol.* 257:H1624–H1633.
Rothberg, B.S., K.S. Shin, P.S. Phale, and G. Yellen. 2002. Voltage-controlled gating at the intracellular entrance to a hyperpolarization-activated cation channel. *J. Gen. Physiol.* 119:83–91.
Sadja, R., K. Smadja, N. Alagem, and E. Reuveny. 2001. Coupling Gβγ-dependent activation to channel opening via pore elements in inwardly rectifying potassium channels. *Neuron.* 29:669–680.
Shyng, S., T. Ferrigni, and C.G. Nichols. 1997. Control of rectification and gating of cloned KATP channels by the Kir6.2 subunit. *J. Gen. Physiol.* 110:141–153.
Shyng, S.L., and C.G. Nichols. 1998. Membrane phospholipid control of nucleotide sensitivity of KATP channels. *Science.* 282:1138–1141.
Tucker, S.J., F.M. Gribble, C. Zhao, S. Trapp, and F.M. Ashcroft. 1997. Truncation of Kir6.2 produces ATP-sensitive K^+ channels in the absence of the sulphonylurea receptor. *Nature.* 387:179–183.
Xiao, J., X. Xhen, and J. Yang. 2003. Localization of PIP_2 activation gate in inward rectifier K^+ channels. *Nat. Neurosci.* 6:811–818.
Xie, L.H., S.A. John, and J.N. Weiss. 2002. Spermine block of the strong inward rectifier potassium channel Kir2.1: dual roles of surface charge screening and pore block. *J. Gen. Physiol.* 120:53–66.
Xie, L.H., S.A. John, and J.N. Weiss. 2003. Inward rectification by polyamines in mouse Kir2.1 channels: synergy between blocking components. *J. Physiol.* 550:67–82.
Yi, B.A., Y.F. Lin, Y.N. Jan, and L.Y. Jan. 2001. Yeast screen for constitutively active mutant G protein-activated potassium channels. *Neuron.* 29:657–667.